IEEE Photonics Journal
An IEEE Photonics Society Publication

Open Access

All-Normal-Dispersion Mode-Locked Fiber Laser With a Tunable Angle-Spliced Polarization-Maintaining Fiber Lyot Filter

Volume 13, Number 3, June 2021

Zhengru Guo
Qiang Hao
Kun Huang
Heping Zeng

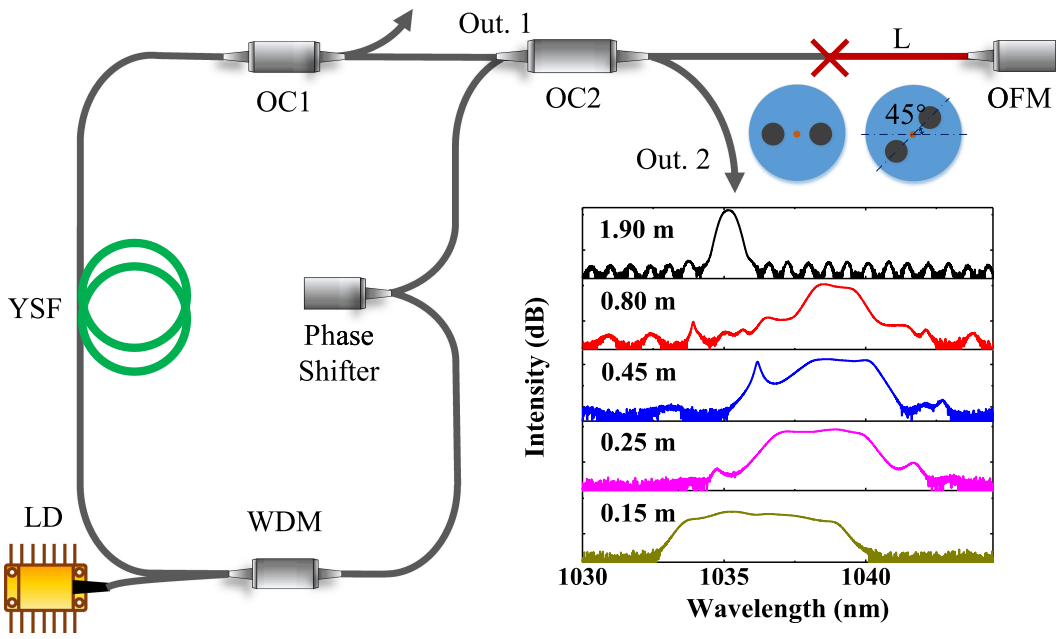

DOI: 10.1109/JPHOT.2021.3079417

All-Normal-Dispersion Mode-Locked Fiber Laser With a Tunable Angle-Spliced Polarization-Maintaining Fiber Lyot Filter

Zhengru Guo [1], **Qiang Hao** [2], **Kun Huang** [1], **and Heping Zeng** [1,3,4,5]

[1]State Key Laboratory of Precision Spectroscopy, East China Normal University, Shanghai 200062, China
[2]Shanghai Key Laboratory of Modern Optical System, and Engineering Research Center of Optical Instrument and System, Ministry of Education, School of Optical Electrical and Computer Engineering, University of Shanghai for Science and Technology, Shanghai 200093, China
[3]Chongqing Institute of East China Normal University, Chongqing 401123, China
[4]Jinan Institute of Quantum Technology, Jinan 250101, China
[5]CAS Center for Excellence in Ultra-intense Laser Science, Shanghai 201800, China

DOI:10.1109/JPHOT.2021.3079417

Manuscript received March 17, 2021; revised April 28, 2021; accepted May 9, 2021. Date of publication May 12, 2021; date of current version June 2, 2021. This work was supported by the National Key R&D Program of China under Grant 2018YFB0407100, in part by the National Natural Science Foundation of China under Grant 11727812, and in part by the Shanghai Municipal Science and Technology Major Project under Grant 2019SHZDZX01. Corresponding author: Heping Zeng (e-mail: hpzeng@phy.ecnu.edu.cn).

Abstract: We have proposed and implemented an all-polarization-maintaining mode-locked fiber laser operating in all-normal-dispersion regime based on nonlinear amplifying loop mirror. The required spectral filtering on the circulating chirped pulse was realized with a Lyot filter that was constructed by two carefully angle-spliced polarization-maintaining single-mode fibers within the laser resonator. The intrinsic inline fiber optical filter exhibited desirable features such as compact layout, adjustable versatility, and long-term stability. By changing the specific fiber length, our laser could deliver pulses with spectral bandwidth from 0.5 to ~4 nm. Furthermore, a continuously tunable single-wavelength operation and an asynchronous dual-wavelength operation can both be obtained with the laser setup including an improved Lyot filter, and the experimental observations agreed well with numerical analysis.

Index Terms: Fiber lasers, Yb-fiber lasers, ultrafast lasers, mode-locked lasers.

1. Introduction

All-normal-dispersion (ANDi) Yb-doped fiber lasers have attracted intensive interests due to the great potential to approach higher power or energy performances [1]–[4]. The involved large chirp induced by the fiber effectively minimizes the nonlinear accumulation and allows high-energy operation. However, without dispersion compensation, the oscillated pulses in the ANDi fiber cavity will be monotonously stretched and thus disenable the convergent mode-locking. Therefore, dispersion management components, such as spectral filters, including the bulk optical components and fiber-integrated devices, are commonly required to realize stable ANDi operations [3], [5]–[7]. Unfortunately, the immutable spectral filter determines the output parameters of the laser, and

imposes a restriction on its flexibility, tunability, and versatility. For example, narrowband lasers centered at 1064.3 nm with $<$1 nm bandwidth are preferred as seeders for the Nd:YVO_4 picosecond (ps) amplifiers [8], but it would not be suitable for the generation of ultra-short pulses with $\sim$200 fs duration [9]. For bio-medical applications, tunable and switchable fiber lasers are widely required for the label-free imaging techniques such as multiphoton microscopy [10] and coherent anti-Stocks Raman scattering [11]. More recently, a single cavity dual-wavelength fiber laser has greatly simplified dual-comb spectroscopy with compact size and cost efficiency [12], but it would be difficult to be realized in a fiber resonator with a single-channel filter.

One possibility to realize the versatile fiber laser is to employ the concept of Lyot filter, which could be realized by a segment of highly birefringent media at an angle of 45° sandwiched in between two polarizers [13]. With a segment of polarization maintaining (PM) fiber replacing the birefringent media, K. Özgören *et al.* constructed an all-fiber Lyot filter inside a laser cavity [14]. The mode-locked operation was guaranteed by nonlinear polarization evolution (NPE) mechanism and Lyot filtering effect. After then, many works have proved the potential of fiber-based Lyot filter in realizing switchable and tunable mode-locked lasers [15]–[17]. However, long-term stability of the NPE based lasers remains unsatisfactory, especially when a segment of PM fiber was introduced to assist the nonlinear polarization evolution [18].

To improve the environmental stability, substantial efforts have been devoted to realizing mode-locked lasers with all-PM fibers. Real saturable absorbers (SAs), including semiconductor SAs [19], carbon-nanotube [20], two-dimensional materials [21], [22], and nanoparticles [23]–[25] have all been applied to realize the mode-locking fiber lasers, and some of them have been implemented in all-PM fiber lasers. However, the real-SAs usually suffer from long-term reliability or poor power-handling capabilities [20]. NPE and nonlinear amplifying loop mirror (NALM) are two conventional artificial SA mechanisms. Several NPE based all-PM fiber lasers have been demonstrated, but they are all delicate designs with low error-tolerance and mild sensitivity [18], [26], [27]. Regarding the NALM based fiber lasers, Jiang and Guo *et al.* have demonstrated the low-threshold, self-started, all-PM fiber lasers operating at dissipative and stretched-pulses solitons regimes, respectively[28], [29]. In their schemes, fiber type bandpass filters, gratings, or bulk birefringent crystals are essential elements for mode-locking, resulting in additional complexity and low tolerance of environmental disturbance.

Here, we combined the NALM technique with the Lyot filtering effect to realize a long-term stable ANDi fiber laser. By angle splicing two segments of PM fibers, a reflection type PM Lyot filter which replaces the conventional filter for dispersion management is demonstrated. The Lyot filter endows the laser setup no only compactness and robustness but also flexibility in controlling the output spectral bandwidth and pulse duration. Both numerical analysis and experimental results confirm that. Furthermore, with an improved Lyot filter, the laser setup is enhanced in versatility to deliver tunable single-wavelength pulse train as well as asynchronous dual-wavelength pulse trains.

2. Experimental Details and Principles

Fig. 1 shows the laser configuration, which is built up in a linear cavity and employs a NALM as one end-mirror, and a fiber type reflector as the other end-mirror. A wavelength-division multiplexer (WDM), a phase shifter, a 10:90 fiber coupler (OC1), and a 1.5-m long gain fiber (YSF:Nufern, PM-YSF-HI) make up the NALM. At the other end, an optical fiber mirror (OFM) is angle-spliced with the pigtail fiber of OC2 to form the linear arm, meanwhile, to act as the Lyot filter. The NALM and linear arm sandwich a 50:50 fiber coupler (OC2) to complete the resonant cavity. A 976 nm laser diode (LD) with a maximum output power of 400 mW is used as the pumping source. Among the fiber components, two couplers (OC1 and OC2) and WDM are slow axis working (fast axis blocking) devices, and all the fiber pigtails are spliced by a PM fusion splicer. Output pulses extracted from OC1 (Out. 1) and OC2 (Out. 2) serve as the output and monitor laser, respectively.

For a simple and clear investigation on the Lyot filter, we use a pair of collimators to improve the linear arm, as shown in Fig. 1(b). The two collimators are well aligned with a coupling efficiency of 90%. Among them, COL1 is fixed, and COL2 is placed on a rotatable plate to adjust the angle

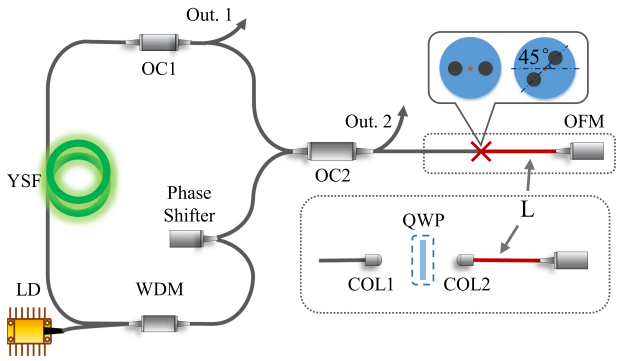

Fig. 1. (a) Experimental configuration of the laser. LD: laser diode; WDM: wavelength division multiplexer; YSF: Yb-doped single-mode fiber; OC1: fiber coupler with 10:90 splitting ratio; OC2: fiber coupler with 50:50 splitting ratio; OFM: optical fiber mirror. (b) The improved configuration of the linear arm. COL1 and COL2: collimators; QWP: quarter-wave plate. QWP is not incorporated at first. The fiber marked in red is referred as specific fiber in the text.

TABLE 1
Jones Matrices of Optical Elements

Optical elements	Jones Matrix	Parameters	Abbreviation
PM fiber	$\begin{pmatrix} e^{i\phi} & 0 \\ 0 & e^{-i\phi} \end{pmatrix}, \phi = \frac{\pi BL}{\lambda}$	B is the birefringence of PM fiber, L is the length of spliced PM fiber between COL2 and OFM, λ is wavelength of pulse trains.	J_{PMF}
Rotating matrix	$\begin{pmatrix} Cos[\theta] & -Sin[\theta] \\ Sin[\theta] & Cos[\theta] \end{pmatrix}$	θ is the angle difference between COL1 and COL2. β is the rotating angle of incident QWP	$J_{[\theta]}$, $J_{[\beta]}$,
OFM	$\begin{pmatrix} 1 & 0 \\ 0 & -1 \end{pmatrix}$		R
QWP	$\begin{pmatrix} 1 & 0 \\ 0 & -i \end{pmatrix}$		J_{QWP}

difference between the principle axes of the two PM collimators. The initial fiber length (L) between COL2 and OFM is set to 0.8 m. By changing the angle difference, extending or tailoring the fiber, and inserting a rotatable QWP, we can engineer the fiber laser to perform rich kinds of mode-locking states.

We firstly perform numerical analysis on the PM Lyot filter by using the Jones matrices, where the optical elements' Jones matrices are listed in TABLE 1. Assuming the Jones matrix of the incident pulses is expressed by $\overrightarrow{E_I} = \begin{pmatrix} 1 \\ 0 \end{pmatrix}$. When the incident light propagates through COL2, PM fiber, OFM and received by COL1 again, the transmission Jones matrix ($\vec{T}$) could be expressed through successively multiplying the Jones matrices of each optical element:

$$\vec{T} = J_{[\theta]} * J_{PMF} * R * J_{PMF} * J_{[-\theta]}. \tag{1}$$

Since OC2 is a slow axis working device, the vertical component of the returning light will be completely extinguished. $\overrightarrow{E_{O1}}$ represents the output light, so the final transmission function of the PM Lyot filter is derived as

$$T = \frac{\left|\overrightarrow{E_{O1}}^2\right|}{\left|\overrightarrow{E_I}^2\right|} = 1 - sin2\,(2\theta)\,cos2\,(2\pi BL/\lambda)\,. \tag{2}$$

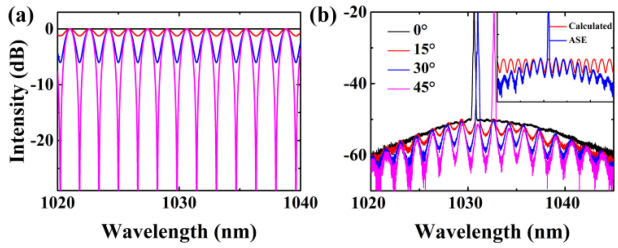

Fig. 2. (a) Calculated transmission curves of the PM Lyot filter with different rotating angles. (b) The recorded ASE spectral curves with different rotating angles. The inset shows the comparison of the calculated transmission curve and the ASE spectral curve at the angle difference of 30°.

Obviously, the angle-aligned linear arm and OC2 co-work to form the Lyot filter that imposes a periodically filtering effect on the optical wavelength of the incident light. Here, we ignore the nonlinear effects since the continuous wave or picosecond pulses induced nonlinear birefringence variation is difficult to reach the magnitude of the intrinsic linear birefringence of the PM fibers. The pass-band spacing is determined by $\Delta\lambda = \lambda^2/2BL$. The PM fiber we used in the cavity is standard PM980 fiber (PM980-XP, Nufern), which has a birefringence (B) of $3.6\sim6.5\times10^{-4}$. When $L = 0.80$ m and $B = 4.1\times10^{-4}$, transmission curve of the PM Lyot filter is plotted in Fig. 2(a). The calculated $\Delta\lambda$ is about 1.6 nm at 1030 nm, and the modulation depth depends on the angle difference between the principle axes of the two collimators. As the angle difference increases from 0° to 45°, $\Delta\lambda$ stays the same, but the modulation depth increases from 0 dB to >25 dB, as the curves shown in Fig. 2(a).

Furthermore, we fixed the angle difference between the two collimators to 45°, and inserted a QWP between them. The improved transmission coefficient T' of the Lyot filter could be recalculated as

$$T' = 1 - cos^2\left[\frac{2\pi BL}{\lambda} + 2\beta\right]. \tag{3}$$

In this equation, β is the rotated angle of QWP, which introduces a phase modulation to T'. The corresponding angle period is 180°. In the spectral domain, the extra phase results in the wavelength shift of the spectral peak. Predictably, the improved Lyot filter will endow the fiber laser a wavelength tunability on the output spectrum.

In experiment, we evaluate the Lyot filtering effect by checking on the output spectrum of the laser. Firstly, with a moderate pumping power of 80-mW, the laser delivers amplified spontaneous emission (ASE) without Q-switching or mode-locking pulses. The output spectra of the ASE obtained from OC1 are recorded by an optical spectrum analyzer (AQ6370D), as shown in Fig. 2(b). The fiber length between COL2 and OFM is set to 0.8 m. When the two collimators are precisely aligned without angle difference, the recorded output spectrum (the black curve) shows no periodical fluctuation except an intrinsic amplitude envelope stems from the emission of Yb^{3+} ions. The modulation depth of the obtained output spectra increased with the angle difference. When the angle difference is increased to 45°, the modulation depth is optimized to 13.4 dB (Fig. 2(b), pink curve). The inset of Fig. 2(b) compares the calculated transmission curve and the spectral curve of ASE at the angle difference of 30°. As depicted, the practical $\Delta\lambda$ and modulation depth of the Lyot filter match well with the calculated results.

Next, we turn to achieve the mode-locked fiber laser with the help of the Lyot filter. The pigtails of OC2 and OFM are spliced together with an angle difference of 45°. When the pump power is increased to 240-mW, multi-pulse mode-locking is initiated. By slowly decreasing the pump power to ~70-mW, we can transfer the multi-pulse operation to single-pulse operation. The average output power is about 2-mW due to the low-threshold mode-locking. Fig. 3 shows the output characteristics of the mode-locked pulses with different fiber lengths. As the blue scatters shown in Fig. 3(a), when the specific fiber length of L is reduced from 1.9 m to 0.15 m, the spectral bandwidth is

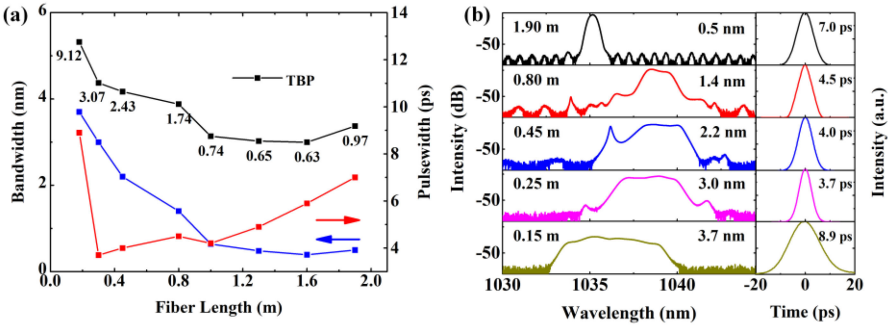

Fig. 3. Output characteristics of the mode-locked pulses with different fiber lengths. (a) Spectral bandwidth (blue scatters), temporal pulsewidth (red scatters), and TBP (black scatters) versus the specific fiber length, and (b) output spectra (left column) and auto-correlation traces (right column).

increased from 0.5 nm to 3.7 nm (the obtained maximum spectral width). The restriction in further extending the spectral coverage is induced by the PM fusion machine, where is difficult for us to implement the splicing process when the fiber pigtails are shorter than 7 cm. Using PM fiber with lower birefringence is possible to get the spectral coverage broader.

In the time domain, as the fiber length is reduced, output pulsewidth and product of time-bandwidth (TBP) of the mode-locked pulses decrease first and then increase, as the red and black scatters shown in Fig. 3(a), respectively. The combination effect of SA, spectral filtering, and fiber dispersion results in the complex evolution of pulsewidth and TBP [30]. When the specific fiber length is longer than 1.0 m, the output pulse has a spectral bandwidth narrower than 0.7 nm, which minimizes the influence of fiber dispersion. Thus, the output pulsewidth is dominated by the filtering and SA effects, and the corresponding TBP is close to that of the transform limited pulse. The output pulse duration with 1.9, 1.6, 1.3 and 1.0 m fiber is 7.0, 5.9, 4.9, and 4.2 ps, respectively. As we proceed to tailor short the fiber, the obtained mode-locked pulse has a spectral bandwidth of more than 1.0 nm. Due to the relatively broad spectral coverage, the fiber dispersion results in the pulse stretching. Consequently, TBPs of the pulses severely increase to be more than three times that of the transform-limited pulse. That is a typical feature of the ANDi fiber lasers.

Fig. 3(b) shows the spectral curves and auto-correlation traces of the mode-locked pulses with some typical fiber lengths. As the fiber length decreases from 1.90 to 0.15 m, center wavelength of the output spectrum shifts first to red and then blue. Owing to the multi-channel nature of the Lyot filter, the center wavelength of the output pulses is determined by co-work of the gain competition and spectral location of the pass-band. When the specific fiber is 1.9 m long, $\Delta\lambda$ of the Lyot filter is 0.7 nm, which makes the gain competition drastic when the pump is turned on. In this situation, the laser is prone to initiate the mode-locking nearby the emission peak (1032 nm) of the gain fiber. In other conditions, $\Delta\lambda$ increases as the fiber length decreasing. The spectral location of the comb filter dominates the output center wavelength to continuously blue-shift.

When we changed the specific fiber length, the rest part of the laser is kept unchanged with a total fiber length of 8.5 m. With either fiber length, the laser shows improved environmental stability than the previously proposed all PM NPE operations, which are not fully environmental stable due to the inaccurate fiber length induced superfluous wave-plate effect [17]–[19]. Fig. 4 depicts the repetition rate fluctuations of the laser with 1.90, 0.80, 0.45, 0.25, and 0.15-m long specific fiber within 10 hours. The respectively maximum jitter of the repetition rate is calculated as 240, 90, 130, 280, and 190 Hz. During the test, no shield was used to protect our laser, so the large fluctuation of the repetition rate is induced by the thermo changes. The laser is stable enough to resist shake or pat on any pieces of the fiber owing to the all PM structure.

To further explore the versatility of the laser, we improved the linear arm as shown in Fig. 1(b). The angle difference between the axes of the two collimators is adjust to 45°, and the specific

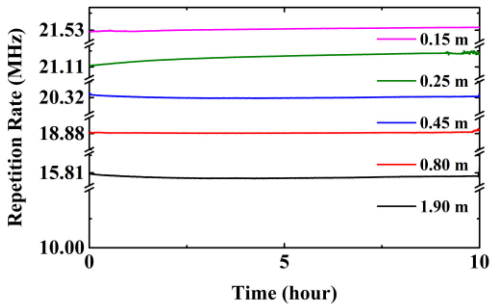

Fig. 4. Fluctuations of the pulse repetition rate with 1.90, 0.80, 0.45, 0.25, and 0.15-m long specific fiber within 10 hours.

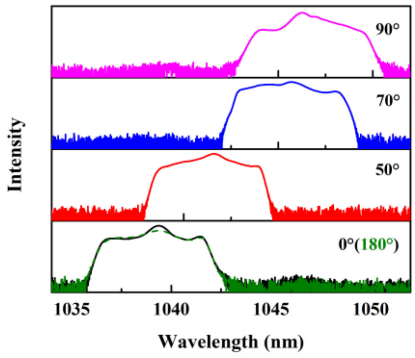

Fig. 5. Wavelength tuning ability of the laser with the improved Lyot filter.

fiber length is set to 0.15 m. With adequate pump power to maintain the mode-locking state, we can regularly and periodically adjust the output spectrum by rotating QWP, as the curves shown in Fig. 5. When QWP is rotated by 90°, center wavelength of the mode-locked pulses red-shifts from 1039 nm to 1047 nm, smoothly. Further increasing the rotation angle to 180°, the tuning path reverses. Since the Lyot filter is akin to a comb filter, the tuning range is restricted by the spectral separation between the adjacent combs, which is about 8 nm. These results well confirmed our numerical analysis. With other fiber lengths, the spectrum tuning could also be observed, but the moderate tuning range makes it inconspicuous.

Additionally, by carefully optimizing the cavity, the laser is capable of delivering dual-wavelength mode-locked pulses as shown in Fig. 6. When the total cavity length is $\sim$7 m and the specific fiber length is $\sim$0.43 m, output spectra of the switchable single-wavelength operations center at 1039.4 and 1042.3 nm, with a spectral bandwidth of 2.1 and 1.9 nm, respectively. Correspondingly, radio frequency (RF) spectral peaks of the single-wavelength operations locate at 26.842 and 26.843 MHz, respectively. As for the dual-wavelength operation, the optical spectrum is a combination of the two single-wavelength operation's and the RF spectrum has two isolated peaks, as the black curves shown in Fig. 6(a) and (b), respectively. The repetition rate difference between the two single-wavelength or dual-wavelength pulses trains is about 740 Hz. The subsidiary two RF peaks are the comb lines originated from the optical interference among the spectral overlap of the dual-wavelength pulses. Fig. 6(c) shows the interferogram of the dual-wavelength pulse trains with a time range of 4 ms. A beat signal with an interval of 1351 μs is observed. It agrees well with the repetition rate difference of $\sim$740 Hz and demonstrates the asynchronous nature of the dual-wavelength operation.

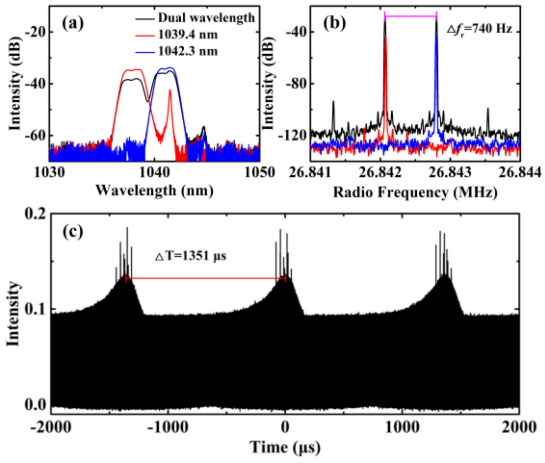

Fig. 6. Output spectral curves (a) and RF spectral curves (b) of the switchable single-wavelength operations and the dual-wavelength operation. (c) The interferogram of the asynchronous dual-wavelength pulses.

3. Discussions and Conclusion

During the experiment, we find that the fiber length between COL1 and OC2 is a crucial factor for the laser to perform satisfactory long-term stability and reliability. The reason should be explained as follows: due to the angle difference with respect to PM fiber axes, when the incident pulses enters the following fiber, it decomposes into two pulses with orthogonal polarizations and then periodically evolves over the multiple beat length [23]. In this situation, longer fiber will magnify the environmental perturbations induced polarization inconsistency, and result in the mode-locking instability.

As for the dual-wavelength mode-locking, we can always obtain asynchronous dual-wavelength pulse trains when the specific fiber length in the Lyot filter is within 25-45 cm. With other lengths, stable dual-wavelength mode-locking could not be observed. Therefore, appropriate pass-band spacing of the Lyot filter is a key factor to guarantee the dual-wavelength oscillation. When the pass-band is too narrow, drastic gain competition results in a degrade on the self-starting ability of the laser, let along the dual-wavelength mode-locking. In contrary, when the pass-band is too broad, the laser is stable enough to output spectral tunable pulses rather than the dual-wavelength pulses.

In conclusion, we have experimentally demonstrated a NALM based ANDi laser in all PM fiber structure. To achieve the compact, stable, and versatile fiber laser, the indispensable bandpass filter used for dispersion management is replaced by an angle-spliced PM Lyot filter. The output parameters of the laser, including spectral bandwidth and pulsewidth can be altered by simply changing the specific fiber length in the Lyot filter. Narrowband or broadband pulses with 0.5-3.7 nm bandwidth have been realized with the laser to enable picosecond or femtosecond pulse amplification. Additionally, with the improved Lyot filter, which including two angle-aligned collimators and a sandwiched QWP, the laser can output tunable single-wavelength pulse train or asynchronous dual-wavelength pulse trains. More possibilities and improved capabilities of the laser such as broader spectral coverage, wider tuning range *et al.* are still under studying. For this work, we believe that our research paves a new way towards the practical, versatile, and cost-effective fiber lasers, and the applications can be promoted to abundant areas such as micromachining, nonlinear imaging, and spectroscopy.

Acknowledgment

The authors would like to thank the anonymous reviewers for their valuable suggestions.

References

[1] B. Oktem, C. Ülgüdür, and F. Ö. Ilday, "Soliton–similariton fibre laser," *Nature Photon.*, vol. 4, pp. 307–311, 2010.
[2] A. Chong, W. H. Renninger, and F. W. Wise, "All-normal-dispersion femtosecond fiber laser with pulse energy above 20nJ," *Opt. Lett.*, vol. 32, pp. 2408–2410, 2007.
[3] A. Chong, J. Buckley, W. Renninger, and F. Wise, "All-normal-dispersion femtosecond fiber laser," *Opt. Exp.*, vol. 14, pp. 10095–10100, 2006.
[4] P. Grelu, and N. Akhmediev, "Dissipative solitons for mode-locked lasers," *Nature Photon.*, vol. 6, pp. 84–92, 2012.
[5] A. Chong, W. H. Renninger, and F. W. Wise, "Environmentally stable all-normal-dispersion femtosecond fiber laser," *Opt. Lett.*, vol. 33, pp. 1071–1073, 2008.
[6] A. Chong, W. H. Renninger, and F. W. Wise, "Properties of normal-dispersion femtosecond fiber lasers," *J. Opt. Soc. Amer. B*, vol. 25, pp. 140–148, 2008.
[7] W. H. Renninger, A. Chong, and F. W. Wise, "Dissipative solitons in normal-dispersion fiber lasers," *Phys. Rev. A*, vol. 77, 2008, Art. no. 023814.
[8] M. Lührmann *et al.*, "High-average power Nd: YVO4 regenerative amplifier seeded by a gain switched diode laser," in *Proc. SPIE - Int. Soc. for Opt. Eng.*, 2011, Art. no. 7912.
[9] A. Pugžlys *et al.*, "Multi-mJ, 200-fs, cw-pumped, cryogenically cooled, Yb,Na:CaF_2 amplifier," *Opt. Lett.*, vol. 34, pp. 2075–2077, 2009.
[10] W. Liu, S. H. Chia, H. Y. Chung, R. Greinert, F. X. Kartner, and G. Chang, "Energetic ultrafast fiber laser sources tunable in 1030-1215 nm for deep tissue multi-photon microscopy," *Opt. Exp.*, vol. 25, pp. 6822–6831, 2017.
[11] K. Yang, J. Jiang, Z. Guo, Q. Hao, and H. Zeng, "Tunable femtosecond laser from 965 to 1025 nm in fiber optical parametric oscillator," *IEEE Photon. Technol. Lett.*, vol. 30, no. 7, pp. 607–610, Apr. 2018.
[12] J. Chen *et al.*, "Dual-comb spectroscopy of methane based on a free-running Erbium-doped fiber laser," *Opt. Exp.*, vol. 27, pp. 11406–11412, 2019.
[13] L. B., "Optical apparatus with wide field using interference of polarized light," *C.R. Acad. Sci. (Paris)*, vol. 197, 1933, Art. no. 1593.
[14] K. Özgören, and F. Ö. Ilday, "All-fiber all-normal dispersion laser with a fiber-based lyot filter," *Opt. Lett.*, vol. 35, pp. 1296–1298, 2010.
[15] Y. S. Fedotov, S. M. Kobtsev, R. N. Arif, A. G. Rozhin, C. Mou, and S. K. Turitsyn, "Spectrum-, pulsewidth-, and wavelength-switchable all-fiber mode-locked yb laser with fiber based birefringent filter," *Opt. Exp.*, vol. 20, pp. 17797–17805, 2012.
[16] Z. Zhang, B. Öktem, and F. Ö. Ilday, "All-fiber-integrated soliton–similariton laser with in-line fiber filter," *Opt. Lett.*, vol. 37, pp. 3489–3491, 2012.
[17] A. Khanolkar, X. Ge, and A. Chong, "All-normal dispersion fiber laser with a bandwidth tunable fiber-based spectral filter," *Opt Lett.*, vol. 45, pp. 4555–4558, 2020.
[18] J. Szczepanek, T. M. Kardas, C. Radzewicz, and Y. Stepanenko, "Ultrafast laser mode-locked using nonlinear polarization evolution in polarization maintaining fibers," *Opt Lett.*, vol. 42, pp. 575–578, 2017.
[19] I. Hartl, G. Imeshev, L. Dong, G. C. Cho, and M. E. Fermann, "Ultra-compact dispersion compensated femtosecond fiber oscillators and amplifiers," in *Proc. Conf. Lasers Electro-Opt./Quantum Electron. Laser Sci. Photonic Appl. Syst. Technol., Tech. Dig. (CD)*, Optical Society of America, 2005, Art. no. CThG1.
[20] K. Kieu, and F. W. Wise, "All-fiber normal-dispersion femtosecond laser," *Opt. Exp.*, vol. 16, pp. 11453–11458, 2008.
[21] T. Feng, X. Li, P. Guo, Y. Zhang, J. Liu, and H. Zhang, "MXene: Two dimensional inorganic compounds, for generation of bound state soliton pulses in nonlinear optical system," *Nanophotonics*, vol. 9, pp. 2505–2513, 2020.
[22] J. Feng *et al.*, "2D ductile transition metal chalcogenides (TMCs): Novel high-performance Ag_2S nanosheets for ultrafast photonics," *Adv. Opt. Mater.*, vol. 8, 2020, Art. no. 1901762.
[23] Y. Zhang *et al.*, "PbS nanoparticles for ultrashort pulse generation in optical communication region," *Part. Part. Syst. Characterization*, vol. 35, 2018, Art. no. 1800341.
[24] X. Li, J. Feng, W. Mao, F. Yin, and J. Jiang, "Emerging uniform Cu_2O nanocubes for 251st harmonic ultrashort pulse generation," *J. Mater. Chem. C*, vol. 8, pp. 14386–14392, 2020.
[25] J. Feng, X. Li, G. Zhu, and Q. J. Wang, "Emerging high-performance SnS/CdS nanoflower heterojunction for ultrafast photonics," *ACS Appl. Mater. Interfaces*, vol. 12, pp. 43098–43105, 2020.
[26] Y. Wang, L. Zhang, Z. Zhuo, and S. Guo, "Cross-splicing method for compensating fiber birefringence in polarization-maintaining fiber ring laser mode locked by nonlinear polarization evolution," *Appl. Opt.*, vol. 55, pp. 5766–5770, 2016.
[27] J. Zhou, W. Pan, X. Gu, L. Zhang, and Y. Feng, "Dissipative-soliton generation with nonlinear-polarization-evolution in a polarization maintaining fiber," *Opt. Exp.*, vol. 26, pp. 4166–4171, 2018.
[28] T. Jiang, Y. Cui, P. Lu, C. Li, A. Wang, and Z. Zhang, "All PM fiber laser mode locked with a compact phase biased amplifier loop mirror," *IEEE Photon. Technol. Lett.*, vol. 28, no. 16, pp. 1786–1789, Aug. 2016.
[29] Z. Guo, Q. Hao, S. Yang, T. Liu, H. Hu, and H. Zeng, "Octave-spanning supercontinuum generation from an NALM mode-locked yb-fiber laser system," *IEEE Photon. J.*, vol. 9, 2017, Art. no. 1600507.
[30] M. Baumgartl, J. Abreu-Afonso, A. Díez, M. Rothhardt, J. Limpert, and A. Tünnermann, "Environmentally stable picosecond yb fiber laser with low repetition rate," *Appl. Phys. B*, vol. 111, pp. 39–43, 2012.